

# Observation of ethanol-induced condensation and decondensation processes at a single DNA molecular level in microfluidic devices equipped with a rapid solution exchange system

Suzuki, Hiroshi

Department of Biomolecular Engineering, Graduate School of Engineering, Nagoya University

Fujiyoshi, Kentaro

Department of Biomolecular Engineering, Graduate School of Engineering, Nagoya University

KAJI, Noritada

Department of Applied Chemistry, Graduate School of Engineering, Kyushu University

Tokeshi, Manabu

Institute of Nano-Life-Systems, Institutes of Innovation for Future Society, Nagoya University

他

<https://hdl.handle.net/2324/7160849>

---

出版情報 : Analytical Chemistry. 92 (13), pp.9132-9137, 2020-06-02. American Chemical Society  
バージョン :  
権利関係 :

# OBSERVATION OF ETHANOL-INDUCED CONDENSATION AND DECONDENSATION PROCESSES AT A SINGLE DNA MOLECULAR LEVEL IN MICROFLUIDIC DEVICES EQUIPPED WITH A RAPID SOLUTION EXCHANGE SYSTEM

Hiroshi Suzuki<sup>†</sup>, Kentaro Fujiyoshi<sup>†</sup>, Noritada Kaji<sup>‡,§,\*</sup>, Manabu Tokeshi<sup>§,||</sup>, Yoshinobu Baba<sup>†,§,⊥,#</sup>

<sup>†</sup>Department of Biomolecular Engineering, Graduate School of Engineering, Nagoya University, Furo-cho, Chikusa-ku, Nagoya 464-8603, Japan

<sup>‡</sup>Department of Applied Chemistry, Graduate School of Engineering, Kyushu University, 744 Motooka, Nishi-ku, Fukuoka 819-0395, Japan

<sup>§</sup>Institute of Nano-Life-Systems, Institutes of Innovation for Future Society, Nagoya University, Furo-cho, Chikusa-ku, Nagoya 464-8603, Japan

<sup>||</sup>Division of Applied Chemistry, Faculty of Engineering, Hokkaido University, Kita-13, Nishi-8, Kita-Ku, Sapporo 060-8628, Japan

<sup>⊥</sup>Institute of Quantum Life Science, National Institutes for Quantum and Radiological Science and Technology, Chiba, 263-8555, Japan

<sup>#</sup>School of Pharmacy, College of Pharmacy, Kaohsiung Medical University, 100, Shih-Chuan 1st Rd., Kaohsiung, 807, Taiwan, R.O.C.

\*Corresponding author: kaji@cstf.kyushu-u.ac.jp

---

**ABSTRACT:** Conformational transitions from secondary (e.g., B to A-form DNA) to higher order (e.g., coil to globule) transitions play important roles in genome expression and maintenance. Several single-molecule approaches using microfluidic devices have been used to determine the kinetics of DNA chromatin assembly because microfluidic devices can afford stretched DNA molecules through laminar flow and rapid solution exchange. However, some issues, particularly the uncertainty of time 0 in the solution exchange process, are encountered. In such kinetic experiments, it is critical to determine when the target solution front approaches the target DNA molecules. Therefore, a new design for a microfluidic device is developed that enables the instantaneous exchange of solutions in the observation channel, allowing accurate measurements of DNA conformational transitions; stepwise, ethanol-induced conformational transitions are revealed. Although full DNA contraction from coil to globule is observed with >50% ethanol, no outstanding change is observed at concentrations <40% in 10 min. With 50% ethanol solution, the DNA conformational transition passes through two steps, (i) fast and constant-velocity contraction and (ii) relatively slow contraction from the free end. The first process is attributed to the B to A conformational transition by gradual dehydration. The second process is due to the coil-globule transition as the free end of DNA starts the contraction. This globular structure formation counteracts the shear force from the microfluids and decelerates the contraction velocity. This real-time observation system can be applied to the kinetic analysis of DNA conformational transitions such as kinetics of chromatin assembly and gene expression.

---

## INTRODUCTION

DNA condensation and decondensation processes play important roles in biological systems, particularly from the viewpoint of data storage because extremely long DNA molecules with sizes of >2 m in *Homo sapiens* have to fold into cell nuclei with sizes of approximately 10  $\mu\text{m}$  in diameter. Histone helps to smoothly condense the DNA molecules into chromatin and decondense (as necessary) for gene expression, cell division<sup>1</sup>, and other processes. These natural condensation processes have attracted significant interest not only in polymer physics but also in pharmaceutical applications in gene delivery systems. Various artificial condensing agents have been explored, such as basic proteins<sup>2, 3</sup>, alcohols<sup>4, 5</sup>, multivalent cations<sup>6, 7</sup>, neutral

molecular crowding polymers<sup>8-10</sup>, and their combination<sup>11, 12</sup>. The development of single-molecule techniques including optical tweezers<sup>13</sup>, atomic force microscopy (AFM)<sup>14, 15</sup>, and microfluidic devices<sup>3, 16-18</sup> has enabled the investigation of the semiflexible properties of DNA molecules under external forces (optical radiation, mechanical, magnetic, or hydrodynamic) through the condensation and decondensation processes. Although the ethanol precipitation technique based on the above condensation and decondensation phenomenon is widely used in DNA purification and the statistical structures have been well studied, the kinetics of the DNA conformational transition induced by ethanol at the single-molecule level has not been thoroughly understood.

Secondary conformational transition of DNA molecules from B to A-form occurs by the removal of the bound water molecules from the phosphate groups of the DNA backbone. Several studies including X-ray crystallography<sup>19, 20</sup>, NMR<sup>21, 22</sup>, dielectric relaxation<sup>23, 24</sup>, and molecular dynamics simulation<sup>25, 26</sup> have demonstrated that a significant amount of water molecules, that is, 18–19 water molecules per nucleotide are bound in the B-form DNA, but only 13–14 water molecules are bound in the A-form DNA<sup>27</sup>. These hydration layers affect the DNA conformation and biofunctionality, but most of the B to A conformational transitions of DNA have been studied using oligonucleotide or short DNA fragments that are up to a few tens of base pairs. Yoshikawa et al. observed the behavior of long DNA molecules with sizes of >10 kbp in highly concentrated ethanol solutions under low-salt conditions, and measured the conformational transition of B to A form and coil to globule by circular dichroism (CD) spectroscopy and fluorescence microscopy, respectively. They found that the higher-order conformational transition, coil to globule, proceeds together with the transition of the secondary structure from B to C and C to A in a cooperative manner<sup>4</sup>. Interestingly, the second higher order conformational transition from globule to the coil state was observed with approximately 70% ethanol solution. Wang et al. performed condensing force measurements in an aqueous ethanol solution using magnetic tweezers and found that the value was  $\leq 0.2$  pN with 50% ethanol, which is significantly lower than those induced by multivalent cations and cationic surfactants<sup>5</sup>. However, the kinetics of the conformational transition processes of long DNA molecules are still unknown, mainly because of the lack of solution exchange systems that can define the exact ethanol concentration at a certain time. A microfluidic device is a strong candidate for real-time kinetic analysis of DNA conformational transition with solution exchange because rapid injection of different solutions that suppresses the concentration change at the solution interface is possible.

In microfluidic devices, the experiments for observing the DNA conformational transition at a single-molecule level generally involve attaching one end of the DNA molecule to a coated surface. Under a controlled flow, the injected solution or molecules such as ethanol or protamine are advected to the immobilized DNA molecules on the surface, and their kinetics are measured quantitatively by real-time visualization. To perform accurate kinetic measurements at a single DNA molecular level, the concentrations of the analytes at the surface and the front of the injected solution are essential. If the analytes are in the Taylor dispersion regime<sup>28</sup>, the concentration at the surface and front can be simply regarded as the bulk concentration. However, in many practical cases of microfluidic experiments using pressure-driven flow, the timescale is too short to satisfy the Taylor regime, and the Taylor's Gaussian diffusivity across the parabolic flow profile in a microchannel is inhomogeneous, particularly close to the surface where the flow velocity decreases to zero. As a result, the uncertainty of the target solution concentration at time 0 as it approaches the target DNA molecule is always observed. Therefore, in these types of kinetic experiments, it is critical to determine when the front of the target solution approaches the target DNA molecules, such that the concentration time lag of Taylor's Gaussian diffusion can be ignored. To prevent these drawbacks and perform rapid solution exchange that is faster than the timescale of the conformational transition in the microfluidic channels, numerous efforts have been made to realize this using pneumatic valves<sup>29</sup>, pinch solenoid valves<sup>30</sup>, T-junction structures<sup>31</sup>, and other devices.

In this study, a precise and rapid solution exchange system ( $\sim 0.5$  s) is developed on a microfluidic chip and the real-time observation of the conformational transition induced by ethanol is achieved. The relationship between secondary and higher-order conformational changes is also established.

## MATERIALS AND METHODS

### Microfluidic device fabrication and microfluidic operation

Polydimethylsiloxane (PDMS)-based microfluidic chips were fabricated using standard soft lithography methods<sup>32</sup>. Photolithographic masks for patterning the microfluidic channels were delineated using a digital printing service (Nagoya University Co-op, Nagoya, Japan) on an OHP transparency film. A negative photoresist, SU-8 (Nippoin Kayaku Co. Ltd., Tokyo, Japan), was spin-coated (IF-D7, Mikasa Co., Ltd., Tokyo, Japan) onto a 3" silicon wafer (Advantec Co. Ltd., Tokyo, Japan) to form a 50- $\mu$ m thick film, according to the procedure described by the supplier. After pre-baking for 10 min at 95 °C, the SU-8 was cured by UV exposure using a photolithographic mask and standard lithography mask aligner (M-1S, Mikasa Co., Ltd., Tokyo, Japan), and then post-baked for 8 min at 95 °C. The cured pattern was developed using SU-8 developer (Nippoin Kayaku Co., Ltd., Tokyo, Japan) and washed with isopropanol (Wako Pure Chemical Industries, Ltd, Tokyo, Japan). The fabricated master mold was silanized in a desiccator, which was filled with trichloro(1H,1H,2H,2H-perfluorooctyl)silane (Sigma-Aldrich Co. LLC., Tokyo, Japan) vapor prior to the addition of a mixture of curing agent and PDMS prepolymer (SYLGARD 184 Silicone Elastomer Kit, Dow Corning Toray Co., Ltd., Tokyo, Japan) in 1:10 weight ratio. The prepolymer mixture was degassed in a vacuum desiccator for 2 h and cured overnight. The PDMS replica was peeled from the master mold, and the reservoirs with diameters of 3 mm were punched. The surface of the PDMS replica was treated using soft plasma etching equipment (SEDE-PFA, MeiwaFosis Co., Ltd., Tokyo, Japan) for 45 s at 5 mA and then bonded with a cover slip (Figure 1a).

To precisely control the flow in the microchannel, an electroosmotic (EO) pump (Nano Fusion Technologies, Inc., Tokyo, Japan) was connected to the inlet and/or the drain ports through a silicon tube, and the flow rate was controlled using a high-voltage power supply (HVS448 1500, LabSmith, Inc., Livermore, CA) (Figure 1b). To supply ethanol solution with the intended concentration into the microchannel, both the indirect and direct pumping methods were employed. For the indirect pumping method, the ethanol solution was filled using an appropriate length of silicon tube and connected between the interfaces of the EO pump and microchannel reservoir prior to applying an electric field to the EO pump.

### DNA preparation

A solution of  $\lambda$ -DNA (Takara Bio Inc., Shiga, Japan) was heated to 65 °C for 5 min followed by rapid cooling before usage to avoid intra and intermolecular ligation. A single-stranded overhang at the end of  $\lambda$ -DNA (Takara Bio Inc., Shiga, Japan) was hybridized with a complementary oligonucleotide with a sequence of 5'-AGG TCG CCG CCC(A)<sub>20</sub>-biotin-3' at 16 °C for 1 h using a DNA ligation kit (Mighty Mix, Takara Bio Inc., Shiga, Japan).  $\lambda$ -DNA was fluorescently labeled with YOPRO-1 iodide (Thermo Fisher Scientific K. K., Tokyo, Japan) at 1:20 dye-to-DNA base pair ratio, and DL-dithiothreitol was added to the DNA solution to prevent photobleaching, with a final concentration of 10  $\mu$ M. The prepared solution was kept in the dark at 4 °C and used for observation within a week.

## DNA observation

Cover slips (Matsunami Glass Ind, Ltd., Osaka, Japan) for DNA observation were washed in piranha solution consisting of 4:1 mixture of concentrated sulfuric acid ( $\text{H}_2\text{SO}_4$ ) and hydrogen peroxide ( $\text{H}_2\text{O}_2$ ) at  $180^\circ\text{C}$  for 2 h. After bonding the PDMS replica and cover slip,  $20\ \mu\text{l}$  of 2 mg/ml biotinylated bovine serum albumin (biotin-BSA, Thermo Fisher Scientific K. K., Tokyo, Japan) in Phosphate-Buffered Saline (PBS) was introduced into the microchannel and incubated for 30 min within the  $15^\circ\text{C} - 20^\circ\text{C}$  range. After flushing the solution,  $20\ \mu\text{l}$  of 0.25 mg/ml streptavidin (Thermo Fisher Scientific K. K., Tokyo, Japan) in PBS was filled in the microchannel for 30 min at room temperature to prepare streptavidin-modified surface for the subsequent DNA immobilization. Twenty microliters of 1% Blocker™ BSA (Thermo Fisher Scientific K. K., Tokyo, Japan) was injected and incubated for 1 h to prevent non-specific adsorption. Finally, the biotin-modified  $\lambda$ -DNA solution was introduced into the microchannel and incubated for 10 min to immobilize one end of the  $\lambda$ -DNA on the cover slip. All the above processes were manually performed using a pipette (Gilson,

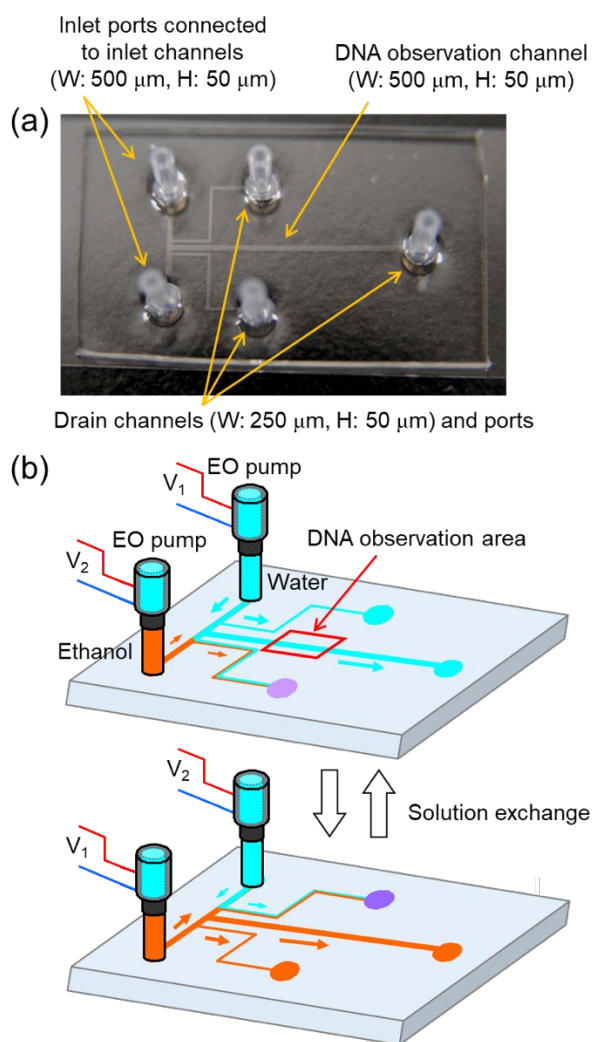


Figure 1. Schematic of the microfluidic device and microfluidic operation by EO pumps. (a) Photograph of the PDMS-based microfluidic device. Short silicone tubes are glued to every reservoir using uncured PDMS for connection to EO pumps and PEEK tubes. (b) Schematic of the principle of solution exchange of water with ethanol solution. Solution with desired concentration is injected by controlling the voltage applied to the EO pumps. The schematic illustrates the solution flow under a voltage condition of  $V_1 > V_2$ .

Middleton, WI). Next, the nozzles of EO pumps filled with MilliQ water or a specific concentration of ethanol solution were inserted into the inlet ports, and DNA observation was performed by controlling the flow rate. Rhodamine B (Sigma-Aldrich Co. LLC., Tokyo, Japan) dissolved in an aqueous ethanol solution at a concentration of  $40\ \mu\text{g}/\text{ml}$  was used to visualize the fluidic flow in the microchannel.

## RESULTS AND DISCUSSION

### Performance of EO pump for solution exchange

To elucidate the performance of the EO pump for this experiment, the flow rates of MilliQ water and 99.5% (v/v) aqueous ethanol solution, and the exchange time of the two solutions were measured. The flow rates were calculated based on the time required for the air–water or air–ethanol interface to pass through a specific distance in a polystyrene tube connected to the EO pump. In general, an indirect pumping system is used for the delivery of ethanol solution because the solution of a poor proton donor cannot generate a sufficient flow rate as a pump. However, in this ethanol-concentration-sensitive experiment, to prevent merging and change in the ethanol concentration at the boundary of ethanol in a connecting tube and water in an EO pump, MilliQ water and 99.5% (v/v) aqueous ethanol solution were filled in both the EO pump and polystyrene tube, respectively, for the flow rate measurements of water and ethanol, respectively. As expected, the flow rate of the ethanol solution is lower, but both the water and ethanol flow rates are linearly proportional to the applied voltage, and their coefficients of determination are 0.998 and 0.997, respectively, as shown in Figure 2. Therefore, for the following experiments, the above-mentioned “direct” pumping system filled with the desired solution was adopted.

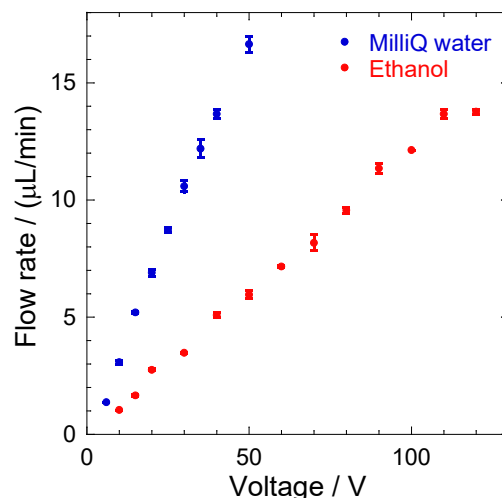


Figure 2. Flow rates of Milli Q water and 99.5% (v/v) aqueous ethanol solution in response to the voltage applied to the EO pump in the microchannel ( $n=3$  for MilliQ water and  $n=2$  for aqueous ethanol solution, where  $n$  is the number of measurements using different microchips). Maximum value of coefficient of variation (CV) was 3.2% at 35 V in Milli Q water and 4.2% at 70 V in 99.5% (v/v) ethanol solution.

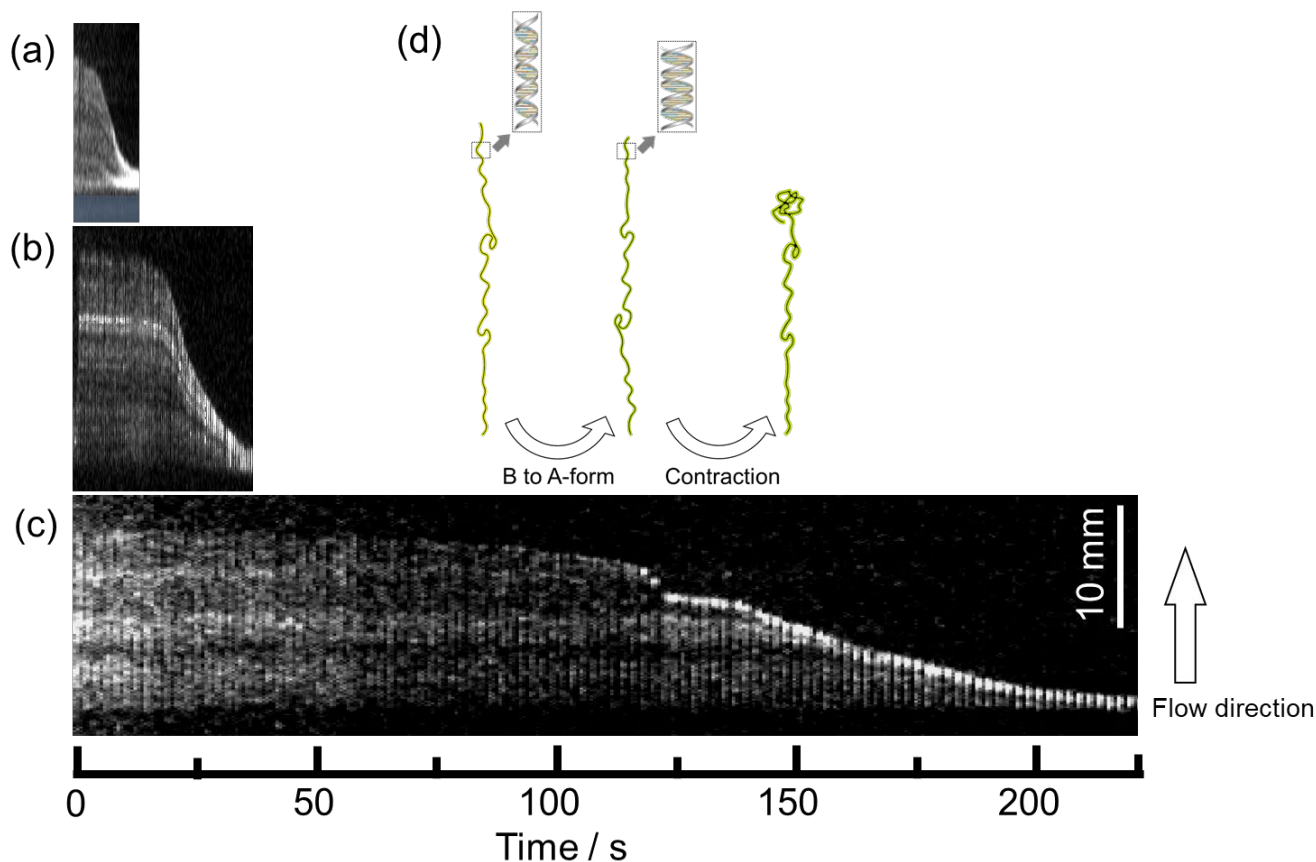


Figure 3. Fluorescence of DNA condensation processes after the solution exchange of water with (a) 70, (b) 60, and (c) 50% (v/v) aqueous ethanol solutions. The bottom of the DNA molecule is anchored to the substrate and the solution flow is applied upward. A still image of a DNA molecule is arrayed horizontally. (d) Schematic illustration of the proposed step-wise contraction mechanism under the dehydrated condition.

An interface between water and ethanol in the microfluidic channel is essential to observe the conformational transition of DNA in specific concentrations of ethanol. Therefore, the time required for the interface to reach the intended location in the observation area was measured (Figures S1 and S2). In the first attempt, two EO pumps were connected to the inlet reservoirs through the tubes (the three outlet reservoirs were “opened”) and the time was measured, but the flow rate was unstable and did not show a linear increment according to the detection distance. For a stable flow rate, three outlet reservoirs were connected to the EO pumps and a constant voltage of 4 V as back pressure was applied; the extruded flow was controlled in conjunction with the pumping flow. The time measurements were performed using different microchips to investigate the interchip reproducibility. As shown in Figures S1(a) and (b), in either case, a stable and reproducible flow rate could not be achieved in the above systems. As an alternative method, 4-cm polyetheretherketone (PEEK) tubes were connected to the three outlet reservoirs to apply constant backpressure. This method worked well, affording a stable flow rate and intrachip reproducibility (Figure S2(a–b)). Therefore, this flow control system was employed in the following experiments, unless specifically mentioned.

A rapid solution exchange system shown in Figure 1 was developed. By controlling the voltage applied to the EO pumps, the solution injected into the observation channel can be easily and rapidly changed from water to ethanol within 0.5 s, as shown in Figure S3. Compared to the previous methods using

valves, which can form the liquid–liquid interface perpendicular to the flow direction, this system can reduce and control the thickness of the diffusion layer at the interface and easily define the relationship between the exact concentration and time required for the visualization of DNA molecules.

#### Condensing and decondensing DNA measurements

By using the rapid solution exchange system on a chip, the condensation and decondensation processes of DNA molecules were observed at a single DNA molecular level. As shown in Figure 3, the kymographs of a  $\lambda$ -DNA molecule stained with YOYO-1 at different ethanol concentrations show the appearance of several visibly bright domains along the stretched DNA, even in the initial state at time 0, which can be attributed to the kinks or folds of the DNA chain under mild flow conditions. Interestingly, despite the ethanol concentrations, these domains do not fluctuate dynamically along the chain during the condensation process, and the stretched DNA appears to uniformly contract, regardless of the kink or folds, except at the downstream end. Based on the microscopic images, it was observed that the downstream-coiled end grew to some extent but did not wind up the stretched domain of the DNA chain from the end. This was clearly different from the compaction induced by the monovalent and divalent cations or protamine and histones<sup>3, 16, 30</sup> in a microfluidic stretched DNA system, that is, retracting from the downstream end or binding point of an intruder, triggering nucleation, followed by growth. The results suggested that the uniform two-dimensional contraction of the DNA chain occurred, followed by three-dimensional condensation from the



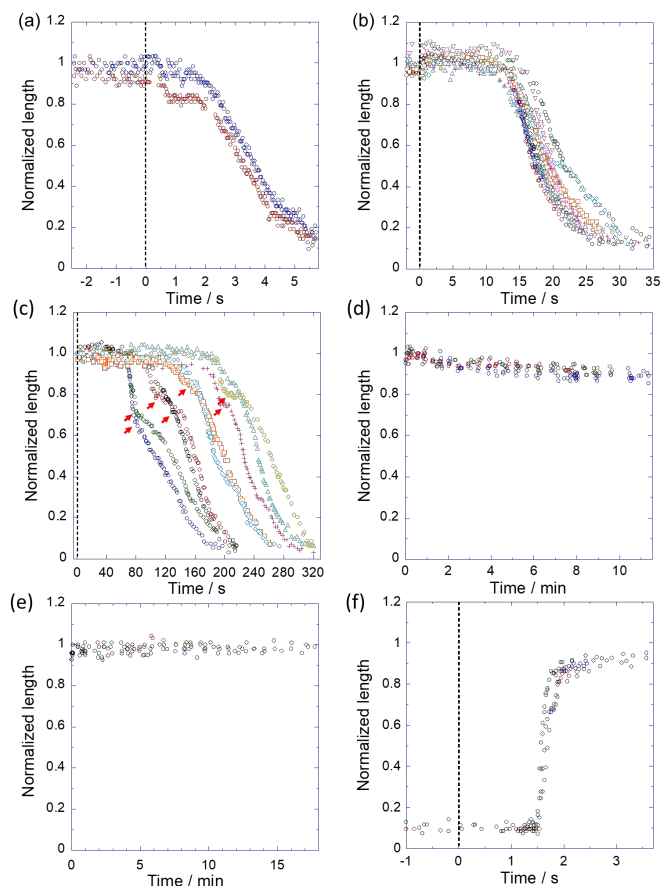


Figure 4. Time course of normalized DNA length before and after solution exchange of MilliQ water with (a) 70%, (b) 60%, (c) 50%, (d) 40%, and (e) 30% aqueous ethanol solutions. The red arrows indicate the turning points. (f) Contracted DNA molecules with 60% ethanol solution are decontracted by injecting water. Time 0 implies the estimated arrival time of the ethanol/water interface at the observed DNA molecules, based on the calibration curve as shown in Fig. S2.

downstream end, after the ethanol solution was exchanged for a few seconds and 2 min with 60% and 50% ethanol, respectively. These observations suggested that the DNA molecules underwent a successive change from B to A-form DNA, followed by a transition of the higher-order structure, that is, coil to compact conformation. The dehydration of water from the surface of the DNA chain suppressed the intramolecular repulsive force and enhanced the conformational transition along the helical axis. Considering the B to A-form DNA contraction ratio of approximately 0.75 ( $=0.26 \text{ nm}/0.34 \text{ nm}$ ), the first rapid and linear contraction could not only be attributed to the B to A-form transition, but also to the progress of twisting and writhing of the DNA chain. Although the DNA molecules in 70% and 60% ethanol solutions appear to be uniformly contracted, as shown in Figures 3(a, b) and 4(a, b), some of the DNA molecules in 50% solution (Figures 3(c) and 4(c)) can show different behaviors, with two or more steps. Most of the molecules show a turning point of the contraction velocity at 0.6–0.8 of the normalized length. The DNA contour length decreases monotonically until this turning point, and then continues to decrease at different velocities. Based on the single-molecule observation, the folding and growth start after the turning point until the globular conformation is formed, corresponding to

completely dehydrated DNA molecules. These stepwise changes can be attributed to the sequential conformational transition of B to A-form and coil to globule transition (Figure 3(d)). As shown in Figure 3(c), the DNA uniformly contracts until approximately 120 s, and then, the free end starts to fold and proceed toward globular formation. This globular structure receives the shear force from the microfluidics, and the shear force gradually increases according to the size of the globule. Therefore, the contraction velocity can change at 0.6–0.8 of the normalized DNA length. In the 40% and 30% ethanol solutions, the DNA contractions are not observed after 10 min, as shown in Figure 4(d), except for a slight contraction (10–15%) in 40% ethanol solution. Although it is difficult to determine if an equilibrium between the water molecules at the surface of the DNA molecule and bulk water molecules is reached within the time-scale ( $\sim 10$  min), it is necessary that the time in a microfluidic system is shorter than that of the normal diffusion-based equilibrium in microtube, e.g., 2-h incubation by Wang *et al.*<sup>5</sup> For observation after 10 min, new methods are required to prevent photobleaching and photocleavage of YOYO-1 stained DNA molecules.

Folded DNA molecules in 60% ethanol are stretched to the coil conformation by introducing water within 1 s, as shown in Figure 4(f). These data reveal the reversible condensation in ethanol solution.

## CONCLUSION

The microfluidic device described in this study can easily generate and control the interface of ethanol and water in the observation channel. As this device does not require valve structures, it can be easily applied to various microfluidic devices that require quick solution exchange. As a model system to study the DNA conformational transitions, ethanol-induced conformational transition is observed using the microfluidic device, and the step-wise conformational transition is successfully investigated. This real-time observation system can allow the kinetic analysis of the DNA conformational transitions such as the kinetics of chromatin assembly.

## ASSOCIATED CONTENT

### Supporting Information

Supporting Information is available free of charge on the ACS Publications website.

Performance of solution exchange system (PDF).

## AUTHOR INFORMATION

### Corresponding Author

Noritada Kaji - Department of Applied Chemistry, Graduate School of Engineering, Kyushu University, Fukuoka 819-0395, Japan; Email: kaji@cstf.kyushu-u.ac.jp

### Author Contributions

All authors have approved the final version of the manuscript.

### Notes

The authors declare no competing financial interests.

## ACKNOWLEDGEMENTS

This work was partially supported by the Japan Science and Technology Agency (JST), PRESTO (No. JPMJPR16F4), the Center of Innovation Program from JST, Nanotechnology Platform Program (Molecule and Material Synthesis) of the Ministry of Education,

Culture, Sports, Science and Technology (MEXT), a JSPS Grant-in-Aid for Scientific Research (A) 24241050, the research grants from IRMAIL science grant, Toshiba Electronic Devices & Storage Corporation, Shimadzu Science Foundation, and Toyota Riken Scholar Program.

## REFERENCES

1. Wood, B. R., The importance of hydration and DNA conformation in interpreting infrared spectra of cells and tissues. *Chemical Society Reviews* **2016**, *45* (7), 1980-1998.
2. Chen, Y.; Zhan, Z.; Zhang, H.; Bi, L.; Zhang, X.-E.; Fu, Y. V., Kinetic analysis of DNA compaction by mycobacterial integration host factor at the single-molecule level. *Tuberculosis* **2019**, *119*, 101862.
3. Ladoux, B.; Quivy, J.-P.; Doyle, P.; Roue, O. d.; Almouzni, G.; Viovy, J.-L., Fast kinetics of chromatin assembly revealed by single-molecule videomicroscopy and scanning force microscopy. *Proceedings of the National Academy of Sciences* **2000**, *97* (26), 14251-14256.
4. Oda, Y.; Sadakane, K.; Yoshikawa, Y.; Imanaka, T.; Takiguchi, K.; Hayashi, M.; Kenmotsu, T.; Yoshikawa, K., Highly Concentrated Ethanol Solutions: Good Solvents for DNA as Revealed by Single-Molecule Observation. *Chemphyschem* **2016**, *17* (4), 471-3.
5. Wang, Y.; Ran, S.; Man, B.; Yang, G., Ethanol induces condensation of single DNA molecules. *Soft Matter* **2011**, *7* (9), 4425-4434.
6. Bloomfield, V. A., DNA condensation by multivalent cations. *Biopolymers* **1997**, *44* (3), 269-82.
7. Oh, Y. S.; Jung, M. J.; Kim, S. K.; Lee, Y. A., Comparison of the Binding Geometry of Free-Base and Hexacoordinated Cationic Porphyrins to A- and B-Form DNA. *ACS Omega* **2018**, *3* (1), 1315-1321.
8. Bloomfield, V. A., DNA condensation. *Current Opinion in Structural Biology* **1996**, *6* (3), 334-341.
9. Crisafulli, F. A. P.; da Silva, L. H. M.; Ferreira, G. M. D.; Ramos, E. B.; Rocha, M. S., Depletion interactions and modulation of DNA-intercalators binding: Opposite behavior of the "neutral" polymer poly(ethylene-glycol). *Biopolymers* **2016**, *105* (4), 227-233.
10. Gu, L.; Zhou, Q.; Zhou, H.; Gao, Q.; Peng, Y.; Song, X.; Liu, Y.; Zhou, X.; Liu, Y., Complex phase transition of DNA condensation under crowding confinement conditions. *Physica A: Statistical Mechanics and its Applications* **2018**, *507*, 489-498.
11. Arscott, P. G.; Ma, C.; Wenner, J. R.; Bloomfield, V. A., DNA condensation by cobalt hexaammine (III) in alcohol-water mixtures: dielectric constant and other solvent effects. *Biopolymers* **1995**, *36* (3), 345-64.
12. Jorge, A. F.; Nunes, S. C. C.; Cova, T. F. G. G.; Pais, A. A. C. C., Cooperative action in DNA condensation. *Current Opinion in Colloid & Interface Science* **2016**, *26*, 66-74.
13. Murayama, Y.; Sakamaki, Y.; Sano, M., Elastic response of single DNA molecules exhibits a reentrant collapsing transition. *Phys Rev Lett* **2003**, *90* (1).
14. Chen, W.-s.; Chen, W.-H.; Chen, Z.; Gooding, A. A.; Lin, K.-J.; Kiang, C.-H., Direct Observation of Multiple Pathways of Single-Stranded DNA Stretching. *Phys Rev Lett* **2010**, *105* (21), 218104.
15. Kenzaki, H.; Takada, S., Partial Unwrapping and Histone Tail Dynamics in Nucleosome Revealed by Coarse-Grained Molecular Simulations. *PLoS computational biology* **2015**, *11*, e1004443.
16. Wagner, G.; Bancaud, A.; Quivy, J. P.; Clapier, C.; Almouzni, G.; Viovy, J. L., Compaction kinetics on single DNAs: purified nucleosome reconstitution systems versus crude extract. *Biophys J* **2005**, *89* (5), 3647-59.
17. Xu, W.; Muller, S. J., Polymer-monovalent salt-induced DNA compaction studied via single-molecule microfluidic trapping. *Lab Chip* **2012**, *12* (3), 647-51.
18. Yeh, J.-W.; Szeto, K., Stretching of Tethered DNA in Nanoslits. *ACS Macro Letters* **2016**, *5* (10), 1114-1118.
19. Schneider, B.; Cohen, D.; Berman, H. M., Hydration of DNA bases: Analysis of crystallographic data. *Biopolymers* **1992**, *32* (7), 725-750.
20. Egli, M.; Tereshko, V.; Teplova, M.; Minasov, G.; Joachimiak, A.; Sanishvili, R.; Weeks, C. M.; Miller, R.; Maier, M. A.; An, H.; Dan Cook, P.; Manoharan, M., X-ray crystallographic analysis of the hydration of A- and B-form DNA at atomic resolution. *Biopolymers* **1998**, *48* (4), 234-252.
21. Jenkins, T. C.; Lane, A. N., AT selectivity and DNA minor groove binding: modelling, NMR and structural studies of the interactions of propamide and pentamide with d(CGCGAATTCGCG)<sub>2</sub>. *Biochimica et Biophysica Acta (BBA) - Gene Structure and Expression* **1997**, *1350* (2), 189-204.
22. Cesare-Marincola, F.; Saba, G.; Lai, A., Optical microscopy and multinuclear NMR investigation of the liquid crystalline netropsin-DNA complex. *Physical Chemistry Chemical Physics* **2003**, *5* (8), 1678-1681.
23. Umehara, T.; Kuwabara, S.; Mashimo, S.; Yagihara, S., Dielectric study on hydration of B-, A-, and Z-DNA. *Biopolymers* **1990**, *30* (7 - 8), 649-656.
24. Son, H.; Choi, D.-H.; Jung, S.; Park, J.; Park, G.-S., Dielectric relaxation of hydration water in the Dickerson-Drew duplex solution probed by THz spectroscopy. *Chemical Physics Letters* **2015**, *627*, 134-139.
25. Samanta, S.; Raghunathan, D.; Mukherjee, S., Effect of temperature on the structure and hydration layer of TATA-box DNA: A molecular dynamics simulation study. *Journal of Molecular Graphics and Modelling* **2016**, *66*, 9-19.
26. Feig, M.; Pettitt, B. M., A molecular simulation picture of DNA hydration around A- and B-DNA. *Biopolymers* **1998**, *48* (4), 199-209.
27. Pal, S. K.; Zhao, L.; Zewail, A. H., Water at DNA surfaces: ultrafast dynamics in minor groove recognition. *Proc Natl Acad Sci U S A* **2003**, *100* (14), 8113-8.
28. Taylor, e. I., Dispersion of soluble matter in solvent flowing slowly through a tube. *Proceedings of the Royal Society of London. Series A. Mathematical and Physical Sciences* **1953**, *219* (1137), 186-203.
29. Unger, M. A.; Chou, H.-P.; Thorsen, T.; Scherer, A.; Quake, S. R., Monolithic Microfabricated Valves and Pumps by Multilayer Soft Lithography. *Science* **2000**, *288* (5463), 113-116.
30. Bancaud, A.; Wagner, G.; Dorfman, K. D.; Viovy, J. L., Measurement of the surface concentration for bioassay kinetics in microchannels. *Anal Chem* **2005**, *77* (3), 833-9.
31. Sachdev, S.; Muralidharan, A.; Boukany, P. E., Molecular Processes Leading to "Necking" in Extensional Flow of Polymer Solutions: Using Microfluidics and Single DNA Imaging. *Macromolecules* **2016**, *49* (24), 9578-9585.
32. McDonald, J. C.; Duffy, D. C.; Anderson, J. R.; Chiu, D. T.; Wu, H.; Schueller, O. J.; Whitesides, G. M., Fabrication of microfluidic systems in poly(dimethylsiloxane). *Electrophoresis* **2000**, *21* (1), 27-40.

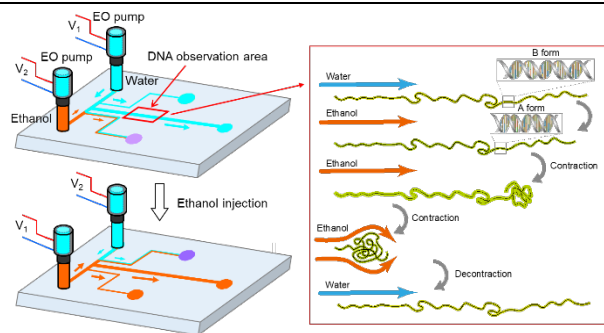


## Table of Contents